Draft version January 23, 2007
Preprint typeset using LaTeX style emulateapj v. 10/09/06

DETERMINING THE NATURE OF DARK MATTER WITH ASTROMETRY

Louis E. Strigari[1,2] James S. Bullock[1], Manoj Kaplinghat[1],

Draft version January 23, 2007

ABSTRACT

We show that measurements of stellar proper motions in dwarf spheroidal galaxies provide a powerful probe of the nature of dark matter. Allowing for general dark matter density profiles and stellar velocity anisotropy profiles, we show that the log-slope of the dark matter profile at about twice the stellar core (King) radius can be measured to within ± 0.2 when the proper motions of 200 stars are added to standard line-of-sight velocity dispersion data. This measurement of the log-slope provides a test of Cold and Warm Dark Matter theories at a sensitivity not possible with line-of-sight velocity dispersion measurements alone. The upcoming SIM PlanetQuest will have the sensitivity to obtain the required number of proper motions in Milky Way dwarf spheroidal galaxies.

Subject headings: Cosmology: dark matter, theory–galaxies: kinematics and dynamics–Astrometry

1. INTRODUCTION

In a Universe dominated by collisionless, Cold Dark Matter (CDM), the central densities of galaxy halos are high, and rise to form cusps with $\rho \sim r^{-1}$, as $r \rightarrow 0$ (Dubinski & Carlberg 1991; Diemand et al. 2005). In contrast, a large class of alternatives to CDM, here generically called Warm Dark Matter (WDM), are expected to have lower central densities and constant density cores at small radii (Dalcanton & Hogan 2001; Kaplinghat 2005; Cembranos et al. 2005; Strigari et al. 2006a). In the majority of WDM models, phase space arguments predict that density cores will be more prominent in lower mass halos. Current observations of the smallest rotationally-supported galaxies are somewhat ambiguous. Some galaxies prefer cored halos, some prefer cusps, and others are well fit by either (Simon et al. 2005; Kuzio de Naray et al. 2006). Moreover, the effects of non-circular motions and other systematic issues are yet to be sorted out for these systems.

The dwarf spheroidal (dSph) satellite galaxies of the Milky Way provide a potentially superior laboratory for studying the nature of dark matter. Observationally, their proximity ($\sim$ 100 kpc) allows kinematic studies of individual stars. Theoretically, their small masses make them ideal candidates for prominent WDM cores. Moreover, the CDM prediction of cuspy central density profiles is robust for these satellite systems because the cusps are stable to any tidal interactions that may have occurred (Kazantzidis et al. 2004). Unfortunately, obtaining dSph density profile slopes has been difficult. The best current constraints on their mass profiles come from analyses of ~ 200 line-of-sight (LOS) velocities (e.g. Łokas et al. 2005; Munoz et al. 2005). The stellar velocity anisotropy is a major source of degeneracy in LOS velocity dispersion modeling, and, as we show below, the log-slope of the underlying density profile remains practically unconstrained even if the number of observed stars is increased by a factor of ~ 10.

In this *Letter*, we examine the prospects of constraining the dark matter density profiles of dSphs by combining stellar LOS velocities with proper motion measurements. We show that ~ 200 proper motions at ~ 5 km s^{-1} accuracy can break the relevant degeneracies and determine the dark matter distribution in the vicinity of the dSph stellar core radius, $r_{\rm king}$. Specifically both the dark halo density and the local log-slope of the dark halo density profile at $\sim 2\, r_{\rm king}$ may be determined with $\gtrsim 5$ times higher precision than from LOS velocity dispersion data alone. Using two well-motivated examples of a cusp and core halo, we show that the local log-slope measurement can distinguish between them at greater than the 3-σ level. We discuss our results in the context of NASA's *SIM PlanetQuest* (Space Interferometry Mission) which will have the sensitivity to measure proper motions of stars at this accuracy in multiple dSphs.

Astrometry as a means to constrain the central density profiles of dSphs was previously considered by Wilkinson et al. (2002). Using a two-parameter family of models for the dSphs, these authors show that proper motions will be enough to completely reconstruct the profile if the underlying shape follows their adopted form. However, CDM halos, and likely their WDM counterparts, are described by a minimum of four unknown parameters: a scale density, a scale radius, an *asymptotic* inner slope, and an *asymptotic* outer slope. By marginalizing over all of these parameters as well as the velocity anisotropy of the stars, we demonstrate that the asymptotic slopes are never well-determined, even with proper motions. We show that what is best constrained is the log-slope, $\gamma(r_*) \equiv -d\ln\rho/d\ln r|_{r=r_*}$, at a radius r_* comparable to the King core radius, specifically $r_* \sim 2\, r_{\rm king}$. We note that unlike the asymptotic $r \rightarrow 0$ slope, the log-slope at $r_* \simeq 0.4$ kpc is known from CDM simulations. This radius corresponds to $\sim 1\%$ of the relevant halo virial radius, and is well-resolved in current simulations.

2. MASS MODELING

We define the three-dimensional (spatial, not projected) components of a star's velocity to be v_r, v_θ, and v_ϕ. The velocity component along the line of sight is then $v_{los} = v_r \cos\theta + v_\theta \sin\theta$, where $\vec{z}\cdot\vec{r} = \cos\theta$ and $\vec{z}$ is the line-of-sight direction. The components parallel and tangential to the radius vector $\vec{R}$ in the plane of the sky are $v_R = v_r \sin\theta + v_\theta \cos\theta$ and $v_t = v_\phi$, respectively.

[1] Center for Cosmology, Dept. of Physics & Astronomy, University of California, Irvine, CA 92697
[2] McCue Fellow

For each component, the velocity dispersion is defined as $\sigma_i^2 \equiv \langle v_i^2 \rangle$. We will assume $\sigma_\theta^2 = \sigma_\phi^2$.

The velocity dispersion for each observed component can be constructed by solving the Jeans equation for the three-dimensional stellar radial velocity dispersion profile $\sigma_r(r)$ and integrating along the line of sight. We note that even in the case of tidally disturbed dwarfs, Klimentowski et al. (2006) have shown that dSph velocity dispersions are well modeled by the Jeans equation, as long as unbound, interloper stars are removed with standard procedures. We derive the three resulting observable velocity dispersions:

$$\sigma_{los}^2(R) = \frac{2}{I_\star(R)} \int_R^\infty \left(1 - \beta \frac{R^2}{r^2}\right) \frac{\nu_\star \sigma_r^2 r dr}{\sqrt{r^2 - R^2}}, \quad (1)$$

$$\sigma_R^2(R) = \frac{2}{I_\star(R)} \int_R^\infty \left(1 - \beta + \beta \frac{R^2}{r^2}\right) \frac{\nu_\star \sigma_r^2 r dr}{\sqrt{r^2 - R^2}}, \quad (2)$$

$$\sigma_t^2(R) = \frac{2}{I_\star(R)} \int_R^\infty (1 - \beta) \frac{\nu_\star \sigma_r^2 r dr}{\sqrt{r^2 - R^2}}. \quad (3)$$

Here $\beta(r) = 1 - \sigma_\theta^2/\sigma_r^2$ is the stellar velocity anisotropy, $I_\star(R)$ is the surface density of stars, and $\nu_*(r)$ is the three-dimensional density of stars. It is clear from inspection that each component depends on β in a different fashion, and therefore can be used together to constrain its value. For $I_\star(R)$ and $\nu_\star(r)$ we use a King profile (King 1962), which is characterized by a core radius, $r_{\rm king}$, and tidal radius, r_t. We adopt values that describe the surface density of Draco: $r_t = 0.93$ kpc and $r_{\rm king} = 0.18$ kpc. Note that the remaining dSphs have similar King concentrations, $r_t/r_{\rm king} \sim 5$, with Sextans having the largest ratio $r_t/r_{\rm king} \sim 10$. Our results do not change significantly as we vary $r_t/r_{\rm king}$ (equivalent to looking at different dSphs).

In Eqs. (1), (2) and (3), the radial stellar velocity dispersion, σ_r, depends on the total mass distribution, and thus the parameters describing the dark matter density profile. We will consider the following general parameterization of the dark matter density profile,

$$\rho(r) = \frac{\rho_0}{(r/r_0)^a [1 + (r/r_0)^b]^{(c-a)/b}}. \quad (4)$$

Here, the value of a sets the *asymptotic* inner slope, and different combinations of b and c set the transition to the asymptotic outer slope. For the specific choice $(a, b, c) = (1, 1, 3)$, we have an NFW profile (Navarro et al. 1996). We denote this as our *cusp* case below. For our *core* case we use $(a, b, c) = (0, 1.5, 3)$, corresponding to a Burkert profile (Burkert 1995). We take these two models to be representative of the predictions of CDM and WDM models. The Burkert profile for the core case is motivated by the expectation that WDM halos will mimic CDM halos at large radius. This was seen in the WDM simulations of Colín et al. (2000). The Burkert choice is also conservative compared to the often-used isothermal core with $(a, b, c) = (0, 2, 2)$, which is more divergent in shape from an NFW and would be easier to distinguish observationally. Regardless, our methods are robust to changes in the underlying form of the density profile.

Eq. (4) allows considerable flexibility in overall form, and the five *shape* parameters (a, b, c, r_0, ρ_0) are in many cases degenerate. However, there are a number of physically relevant quantities that may be derived for any set of the five shape parameters. The first is the log-slope of the dark matter density profile, defined as $\gamma(r) = -d \ln \rho(r)/d \ln r$. For the density profile in Eq. (4) this is given by $\gamma(r) = a - (a - c)(r/r_0)^b/[1 + (r/r_0)^b]$. Other quantities of physical interest are the integrated mass within a given radius, $M(r)$, and the physical density at a given radius, $\rho(r)$, which are clearly obtained for a degenerate set of shape parameters. Below, we show that while the *shape* parameters are not well constrained by dSph velocity data, the *physical* quantities of interest at the scale of the stellar core radius, $r_\star \simeq 2\, r_{\rm king}$, may be constrained to high precision.

3. FORECASTING ERRORS ON PARAMETERS

Our goal is to estimate the accuracy with which the velocity components of stars in dSphs can be used to probe the underlying dark matter distribution. We will consider a model with six independent parameters: a, b, c, ρ_0, r_s, and β = constant. We will consider generalized $\beta(r)$ forms below. In order to keep the profile shape relatively smooth (as is expected for dark matter halo profiles) we restrict the range of b and c by adding Gaussian priors of ± 2.

The errors attainable on these parameters will depend on the covariance matrix, which we will approximate by the 6×6 Fisher information matrix $F_{ij} = \langle \partial^2 \ln \mathcal{L}/\partial p_i \partial p_j \rangle$ (Kendall & Stuart 1969). The inverse of the Fisher matrix, $\mathbf{F}^{-1}$, provides an estimate of the covariance between the parameters, and $\sqrt{F_{ii}^{-1}}$ approximates the error in the estimate on the parameter p_i. The Cramer-Rao inequality guarantees that $\sqrt{F_{ii}^{-1}}$ is the minimum possible variance on the ith parameter for an unbiased estimator. Using $\mathbf{F}^{-1}$ in place of the true covariance matrix involves approximating the likelihood function of the parameters as Gaussian near its peak, so $\mathbf{F}^{-1}$ will be a good approximation to the errors on parameters that are well-constrained. The Fisher matrix also provides information about degeneracies between parameters but obviously should not be trusted for estimates of the error along these degeneracy directions.

We pick large radial bins to compute the velocity dispersions and check that this uncorrelates the different bins. Then the elements of $\mathbf{F}$ are given by

$$F_{ij} = \sum_{M,\ell} \frac{1}{\epsilon_{M\ell}^2} \frac{\partial \sigma_{M\ell}^2}{\partial p_i} \frac{\partial \sigma_{M\ell}^2}{\partial p_j}. \quad (5)$$

The sum is over ℓ radial bins and M refers to the three velocity "methods" – one line-of-sight and two components in the plane of the sky. The errors on the velocity dispersion are represented by $\epsilon_{M\ell}$. We choose bins of equal width in distance, so that there are approximately an equal number of stars in each radial bin. As long as we distribute equal number of stars in each bin, the results we present below are insensitive to the binning scheme, except in the limit of very few bins, or in the limit of small numbers of stars per bin.

To model the errors on the velocity dispersions, we define $\epsilon_{M\ell}^2 = \langle [\sigma_{M\ell}^2 - \langle \sigma_{M\ell}^2 \rangle]^2 \rangle$. We assume that the errors on the velocity of each star are Gaussian and that the theory error (from the distribution function) and experimental error are summed in quadrature,

$$\epsilon_{M\ell}^2 = \frac{2(n-2)}{n^2} \left[{\sigma_{M\ell}^t}^2 + {\sigma_{M\ell}^m}^2 \right]^2, \quad (6)$$

TABLE 1
Fisher Matrix 1-σ errors on parameters.

Parameter	Fiducial Value	Error Quoted	200 LOS + 0 SIM	1000 LOS + 0 SIM	200 LOS + 200 SIM	1000 LOS + 200 SIM	1000 LOS + 500 SIM
$\gamma(r_\star = 2\,r_{\rm king})$	1.3 (0.32)	$\Delta\gamma_\star$	2.0 (2.2)	0.91 (1.0)	0.28 (0.24)	0.21 (0.23)	0.16 (0.15)
$M(r_\star = 2\,r_{\rm king})$ [$10^7 {\rm M}_\odot$]	1.3 (5.3)	$\Delta M_\star/M_\star$	0.27 (0.38)	0.12 (0.17)	0.11 (0.11)	0.07 (0.08)	0.06 (0.05)
$\rho(r_\star = 2\,r_{\rm king})$ [$10^7 {\rm M}_\odot$ kpc^{-3}]	4.0 (2.5)	$\Delta\rho_\star/\rho_\star$	1.6 (0.73)	0.73 (0.33)	0.16 (0.16)	0.13 (0.12)	0.09 (0.09)
$V_{\rm max}$ [km s^{-1}]	22 (28)	$\Delta V_{\rm max}/V_{\rm max}$	1.6 (1.7)	0.71 (0.76)	0.68 (0.93)	0.45 (0.62)	0.38 (0.52)
β	0 (0)	$\Delta\beta$	2.1 (1.4)	0.97 (0.62)	0.16 (0.16)	0.15 (0.15)	0.10 (0.10)
a	1 (0)	Δa	4.4 (4.6)	2.0 (2.1)	0.78 (0.87)	0.55 (0.66)	0.44 (0.51)
ρ_0 [$10^7 {\rm M}_\odot$ kpc^{-3}]	1.0 (3.2)	$\Delta\rho_0/\rho_0$	20 (9.2)	9.1 (4.2)	5.9 (2.0)	4.0 (1.5)	3.3 (1.1)
r_0 [kpc]	2.0 (1.5)	$\Delta r_0/r_0$	8.3 (5.1)	3.8 (2.3)	3.3 (1.8)	2.2 (1.2)	1.8 (1.0)

Note. — Errors refer to the $1-\sigma$ range obtained from a full marginalization over the 6 input parameters $(a, b, c, r_0, \rho_0, \beta)$. Quantities without (with) parenthesis refer to the cusp (core) model described in the text. In the last 5 columns, LOS refers to the number of line-of-sight stars used to derive the quoted errors, and SIM refers to the number proper motions.

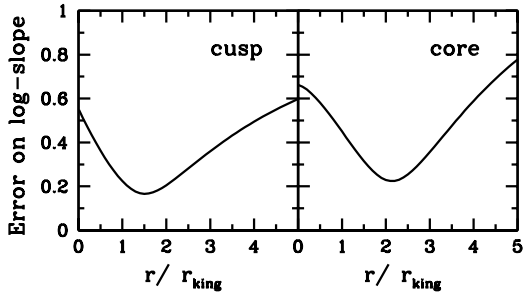

Fig. 1.— The 1-σ error on the log-slope of the density profile as a function of the radius for 1000 LOS velocities combined with 200 proper motions. The *left* and *right* panels show our results for the cusp and core cases, respectively. The value of $r_\star$ is set to be where the error is minimized.

where n is the number of stars in each bin (taken here to be constant from bin to bin). Here σ_ℓ^t is the dispersion in each bin determined from Eqs. (1)-(3), and $\sigma_{M\ell}^m$ represents the measurement error in the velocities of stars in that bin. For LOS velocities, the spectroscopic resolution implies errors $\sigma_{los}^m \sim 1\,{\rm km\,s^{-1}}$, which are negligible compared to the underlying dispersion, $\sigma^t \sim 10\,{\rm km\,s^{-1}}$. SIM can achieve $\sim 10\,\mu$as yr^{-1} proper motions for faint stars [3]. At 100 kpc, this translates to an accuracy of ~ 5 km s^{-1}. We will take this as a typical measurement error for velocities in the plane of the sky.

The derivatives in Eq. (5), and thus the errors attainable on any of the parameters, depend on the location in the true set of parameter space. To examine how the errors vary as a function of the true set of parameters, we choose two fiducial models. Both models produce a "typical" dSph velocity dispersion profile, which is roughly flat at $\sim 10\,{\rm km\,s^{-1}}$ out to r_t. This requirement does not completely fix the profile. For our *cusp* model (NFW) we add the further restriction that r_0 and ρ_0 fall within the expected CDM range (Strigari et al. 2006b). For our *core* model (Burkert) we set r_0 and ρ_0 to give a central phase space density $Q \simeq 10^{-5}\,{\rm M}_\odot\,{\rm pc^{-3}}({\rm km\,s^{-1}})^{-3}$, which can be produced in some WDM models (Strigari et al. 2006a). The values of r_0 and ρ_0 for both models are listed in Table 1 as are the implied log-slopes $\gamma(r_\star) = 1.3$ (cusp) and 0.32 (core) at the characteristic radius $r_\star$, which is set below at the value $2\,r_{\rm king} = 0.36$ kpc.

[3] http://planetquest.jpl.nasa.gov/SIM/sim_AstroIndex.cfm

4. CONSTRAINING THE LOG-SLOPE

The log-slope of the density profile varies with radius, and so does the minimal error attainable on it. We are interested in searching for the radius, $r_\star$, where the log-slope is best constrained. Fig. 1 shows the $1-\sigma$ error on $\gamma(r)$ computed as a function of radius using 1000 line-of-sight velocities and 200 proper motions for the cusp (left) and core (right) models. In both cases, the error reaches a minimum of $\Delta\gamma \simeq 0.2$ at $\sim 2\,r_{\rm king}$ and we explicitly adopt $r_\star = 2\,r_{\rm king}$ for the rest of the discussion. We find that the value of $r_\star$ and the minimum error depend somewhat on the fiducial model. As shown in Fig. 1, profiles with cusps are slightly better constrained than profiles with cores, and $r_\star$ occurs at slightly smaller radii for cusped models. We also find that as $r_t/r_{\rm king}$ increases, the minimum error decreases and $r_\star$ increases. We have chosen a conservatively small ratio here, $r_t/r_{\rm king} \simeq 5$.

Table 1 summarizes our results. We list 1-σ errors attainable on several quantities determined by marginalizing over the 6 fit parameters discussed above. We present errors for five different combinations for the number of LOS stars and proper motion stars. In all cases, the errors on the "physical" parameters, $M(r_\star)$, $\rho(r_\star)$, and $\gamma(r_\star)$, decrease significantly when proper motions are included. Quantities listed without (with) parentheses correspond to the cusp (core) halo case. Note that the errors on the halo shape parameters b and c are essentially the same as the priors we set on them of ± 2 and hence we do not list them in the table.

A quantity that is well constrained without the addition of proper motion information is the mass $M(r_\star)$, which can be determined to 27% (38%) for cusped (cored) models with current data. The mass can be determined to a remarkable $7-8$% accuracy when 200 SIM stars are added. The maximum circular velocity is relatively unconstrained by LOS data alone, but becomes determined to within 45%(62%) for cusped (cored) models with 200 proper motions. More interesting for the nature of dark matter is the log-slope of the density profile at $r_\star$. Even with 1000 LOS velocities, the log-slope in the cusp case is virtually unconstrained, but with the addition of 200 SIM stars the log-slope is well-determined, e.g. $\gamma(r_\star) = 1.3 \pm 0.2$ for the case of an underlying cusp.

The power of velocity dispersions to constrain the density and mass at $r_\star \sim r_{\rm king}$ is relatively simple to understand by examining the observable velocity dispersion components (Eqs. 1, 2 and 3). These

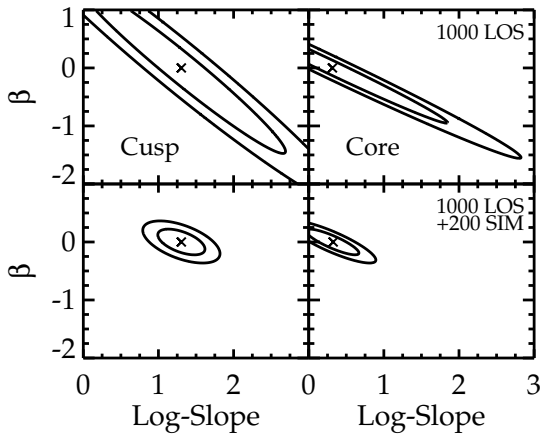

FIG. 2.— The 68% and 95% confidence regions for the dark halo density profile slope measured at $r_\star = 2r_{\rm king}$ and velocity anisotropy β. The left (right) panels correspond to the cusp (core) halo model and the small x's indicate the fiducial values. Upper panels show the errors with 1000 LOS velocities and the bottom panels show the errors for an additional 200 proper motions.

observable quantities depend on the three-dimensional stellar velocity dispersion, which scales as $\sigma_r^2(r) = \nu_\star^{-1} r^{-2\beta} \int_r^{r_t} G\nu_\star(r) M(r) r^{2\beta-2} {\rm d}r \propto r^{2-\gamma_\star}$ for a power-law stellar distribution $\nu_\star(r)$ and constant β. The majority of stars reside at projected radii $r_{\rm king} \lesssim R \lesssim r_{\rm t}$, where the stellar distribution is falling rapidly $\nu_\star \sim r^{-3.5}$. In this case, for $\beta = 0$, the LOS component scales as $\sigma_{los}^2(R) \propto \int_R^{r_t} r^{-0.5-\gamma_\star}(r^2 - R^2)^{-1/2} {\rm d}r$ and is dominated by the mass and density profile at the smallest relevant radii, $r \sim r_{\rm king}$. For $R \lesssim r_{\rm king}$, $\nu_\star \propto r^{-1}$ and σ_{los}^2 is similarly dominated by $r \sim r_{\rm king}$ contributions. Therefore we expect the strongest constraints on the dark matter profile at $r_\star \sim r_{\rm king}$. For $\beta \neq 0$ similar arguments hold but there is a manifest degeneracy between β and the log-slope $\gamma_\star$. As discussed above and illustrated in Table 1, this degeneracy can be broken by including both LOS information (Eq. 1) with tangential information (Eqs. 2, 3).

With the constraints on $\gamma_\star$, are we able to distinguish cored from cusped models? To answer this question, in Figure 2 we present 68% and 95% error contours in the two-dimensional plane of $\gamma_\star$-β. This figure clearly shows the utility of combining both LOS and proper motions. Due to the degeneracy with β, a sample of ~ 1000 line-of-sight stars is unable to distinguish between our two fiducial models, though the models can be clearly distinguished with the addition of proper motions. In the β-$\gamma_\star$ plane, the principal constraining power comes from combining the LOS and R velocity dispersions because the β dependence in these two quantities comes with opposite signs (Eqs. 1, 2).

Finally, we address the fact that β could in principle vary significantly with radius. We have repeated our analysis assuming that $\beta(r) = \beta_0 + \beta_1 r^2/(r^2 + r_\beta^2)$, and marginalize over β_0, β_1 and r_β. We find very small changes to the $\gamma(r_\star)$ error. For reasons similar to those given above, the three different velocity dispersion profiles constrain $\beta(r = r_\star)$ to high accuracy, breaking the β-γ degeneracy.

5. SUMMARY

We have shown that the measurement of proper motions for ~ 200 stars in a typical dSph can be combined with current line-of-sight velocity measurements to constrain the dark halo log-slope to ± 0.2 and normalization to $\pm 15\%$ at about twice the King radius. This is a factor of ~ 5 better than currently possible with LOS velocity dispersion data alone. The results from such observations will provide a very sensitive test of the CDM paradigm and an incisive tool for investigating the microscopic nature of dark matter. We estimate that with ~ 100 days of observing time over the 5 year lifetime of SIM, it will be possible to obtain the proper motions of ~ 200 stars in multiple dSphs (Strigari et al. 2007).

6. ACKNOWLEDGMENTS

We thank S. Kazantzidis, S. Kulkarni, S. Majewski, and R. Munoz for useful discussions. LES is supported in part by a Gary McCue postdoctoral fellowship through the Center for Cosmology at the University of California, Irvine. JSB, LES, and MK are supported in part by NSF grant AST-0607746.

REFERENCES

Burkert, A. 1995, ApJ, 447, L25+
Cembranos, J. A., Feng, J. L., Rajaraman, A., & Takayama, F. 2005, PRL, 95, 181301
Colín, P., Avila-Reese, V., & Valenzuela, O. 2000, ApJ, 542, 622
Dalcanton, J. J. & Hogan, C. J. 2001, ApJ, 561, 35
Diemand, J., Zemp, M., Moore, B., Stadel, J., & Carollo, M. 2005, MNRAS, 364, 665
Dubinski, J. & Carlberg, R. G. 1991, ApJ, 378, 496
Kaplinghat, M. 2005, Phys. Rev. D, 72, 063510
Kazantzidis, S., Mayer, L., Mastropietro, C., Diemand, J., Stadel, J., & Moore, B. 2004, ApJ, 608, 663
Kendall, M. G. & Stuart, A. 1969, The Advanced Theory of Statistics (London: Griffin)
King, I. 1962, AJ, 67, 471
Klimentowski, J., Lokas, E. L., Kazantzidis, S., Prada, F., Mayer, L., & Mamon, G. A. 2006, astro-ph/0611296
Kuzio de Naray, R., McGaugh, S. S., de Blok, W. J. G., & Bosma, A. 2006, ApJS, 165, 461
Łokas, E. L., Mamon, G. A., & Prada, F. 2005, MNRAS, 363, 918
Munoz, R. R. et al. 2005, Astrophys. J., 631, L137
Navarro, J. F., Frenk, C. S., & White, S. D. M. 1996, ApJ, 462, 563
Simon, J. D., Bolatto, A. D., Leroy, A., Blitz, L., & Gates, E. L. 2005, ApJ, 621, 757
Strigari, L. E., Kaplinghat, M., & Bullock, J. S. 2006a, astro-ph/0606281
Strigari, L. E., Kaplinghat, M., Bullock, J. S., Kazantzidis, S., Munoz, R. R., Majewski, S., & Kaufmann, T. 2007, in preparation
Strigari, L. E., Koushiappas, S. M., Bullock, J. S., & Kaplinghat, M. 2006b, astro-ph/0611925
Wilkinson, M. I., Kleyna, J., Evans, N. W., & Gilmore, G. 2002, MNRAS, 330, 778